Photochemistry and Photobiology, 2019, 95: 1258–1266

The Austrian UVA-Network

Alois W. Schmalwieser*[1], Barbara Klotz[2], Michael Schwarzmann[2], Dietmar J. Baumgartner[3], Josef Schreder[4], Günther Schauberger[1] and Mario Blumthaler[2]

[1]Unit of Physiology and Biophysics, University of Veterinary Medicine, Vienna, Austria
[2]Division of Biomedical Physics, Medical University Innsbruck, Innsbruck, Austria
[3]Kanzelhöhe Observatory for Solar and Environmental Research, University of Graz, Graz, Austria
[4]CMS Ing. Dr. Schreder GmbH, Kirchbichl, Austria

Received 30 January 2019, accepted 17 April 2019, DOI: 10.1111/php.13111

ABSTRACT

The ultraviolet-A (UVA) part of the solar spectrum at the Earth's surface is an essential environmental factor but continuous long-time monitoring of UVA radiation is rarely done. In Austria, three existing stations of the UV monitoring network have been upgraded with UVA broadband instruments. At each station, one instrument measures global UVA irradiance and—in parallel—a second instrument measures diffuse irradiance. Recent and past measurements are available via a web page. This paper describes the used instruments, calibration and quality assurance and control procedures. Global and diffuse UVA measurements during a period of up to 5 years are presented. Data indicate clear annual courses and an increase of UVA with altitude by 8–9% per 1000 m. In the first half of the year, UVA radiation is higher than in the second half, due to less cloudiness. In Vienna (153 m asl), the mean daily global UVA radiant exposure in summer is almost as high as at Mt. Gerlitzen (1540 m asl), equalizing the altitude effect, due to less cloudiness. However, in winter, the UVA radiant exposure at Mt. Gerlitzen is double as high, as in Vienna.

INTRODUCTION

The ultraviolet-A (UVA) range (315–400 nm) of the solar spectrum is rarely a topic of continuous monitoring, although UVA is highly important for plants, animals and humans. More common are measurements at certain wavelengths in the UVA range to characterize atmospheric conditions by spectroradiometers (e.g. 1) or narrowband filter radiometers (e.g. 2) and of course most common are measurements of the UV index (e.g. 3). A possible reason for the almost complete lack of UVA monitoring might be that the effects on livings from UVA radiation appear less dramatic than those from the ultraviolet-B (UVB) radiation (e.g. erythema or skin cancer). However, the photobiological and ecological impact of the UVA radiation is as wide as of the UVB radiation.

*Corresponding author email: alois.schmalwieser@vetmeduni.ac.at (Alois W. Schmalwieser)

The visual sense of many animal species is sensitive to UVA radiation, due to an UV sensitive photoreceptor and an UV transmissive lens. Visual perception in the UVA range is long known in invertebrates (4,5) and fish (6,7), was discovered in birds and reptiles in the 1980s (8,9) and has in the meanwhile been even recognized in some mammalian species (e.g. ferret, reindeer (10)). A change of UVA radiation results in a change in the color perception of these animals (11). For farm animals and animals that are kept indoors (e.g. zoo, aviary, terrarium), the availability and quality of UVA radiation are important to ensure their well-being. However, the data available on natural levels of UVA radiation are very limited.

In respect to human and mammalian skin, UVA radiation initiates pigmentation (e.g. 12), which protects the skin from the sun to a certain extent (13), but UVA radiation also contributes effectively to skin aging and wrinkling (14), which may be cosmetically undesirable or even become pathogenic.

Already repeated low exposure to UVA radiation leads to measureable alterations (15,16).

Inside the skin, UVA radiation affects the lipids of cells, which results in a decreased cell metabolism. Furthermore, UVA can generate highly reactive chemical intermediates, such as hydroxyl and oxygen radicals, which can damage DNA. Additionally, UVA radiation is the main trigger for photosensitivity reactions (e.g. phototoxicity and photoallergy (17)). As UVA radiation transmits deeper into the skin (dermis) and into the eye (e.g. 18) than UVB radiation, a significantly larger amount of cells, as well as other tissues (e.g. macular degeneration (19)), can be stroked by photons.

UVA radiation also penetrates more deeply into other mediums like water, plant crops or clothes. For considering UV exposure in everyday life, it has also to be taken into account that glasses (e.g. 20) of windows and windows of vehicles (21) are partially transmissive for UVA radiation. Due to this, people are exposed to UVA radiation, while shielded from UVB radiation.

The amount of UVA radiation reaching the earth's surface is magnitudes greater than that of UVB radiation (e.g. 22). Therefore, UVA radiation makes a significant contribution to photobiological effects (like nonmelanoma skin cancer, cataract (23) or immunosuppression (24)), even if its effectivity is much lower than that of the UVB radiation.

An important vital effect initiated by UVA radiation is photorepair of DNA damage in plants (e.g. 25), but also in microorganisms (e.g. 26). Therefore, the ratio between the damaging

UVB radiation and repairing UVA radiation becomes important. In the case of microorganism, the ratio between photoinactivation and photorepair changes throughout the year (e.g. 27), which may lead to periods which favor the spreading of microorganisms and periods which restrain the spreading. This may result in a reduction or enhancement of airborne infection diseases. There are some hints that the ratio of solar UVB and UVA radiation may be responsible for the spread of influenza A during the winter (28).

Interest in solely measuring UVA radiation was aroused, as the application of UVA radiation became common in phototherapy of certain skin diseases like psoriasis. This happens in conjunction with photosensitizing substances like psoralen. Therefore, several studies were undertaken to investigate the intensity of natural solar UVA radiation for comparison with UVA radiation from artificial sources to avoid overexposure of patients (e.g. 29). Also, in some of the internationally recognized regions for heliotherapy (e.g. psoriasis, atopic dermatitis, vitiligo) like the Dead Sea basin (e.g. 30) or Cyprus (e.g. 31), UVA radiation is a matter of interest.

Another application where UVA radiation measurements are necessary is SODIS (solar water disinfection) (32). SODIS is a low-cost alternative, especially in southern regions, to the disinfection by mercury-vapor-pressure lamps which emit in the more effective UVC and UVB range. Here, irradiance measurements are used to calculate the gained fluence (e.g. 33), respectively, the duration of irradiation needed to ensure disinfection.

A variety of studies focusing on the nature of environmental solar UVA radiation and its influencing factors have been carried out in the past.

It was shown that the spatial variation of sky radiance in the UVA range (e.g. 34) can take a factor of 10. Generally, clouds and aerosols reduce UVA radiation (e.g. 35,36). However, under broken cloud conditions, UVA radiation can be enhanced (e.g. 37), compared to clear sky. Albedo is another influencing factor (e.g. 38) that changes with time (e.g. snow cover). Global UVA radiation increases significantly with altitude (e.g. 39–42). Especially in alpine regions, there is a complex interaction between clouds, albedo and altitude (e.g. 43).

The ongoing global climate change does not affect the biosphere homogeneously. Changes occur on different spatial and temporal scales (e.g. seasonal change of cloud cover) and progress with different speeds. These also affect the amount of incoming UV radiation and its biological effectiveness (e.g. 44). Reliable long-term monitoring is necessary in conjunction to a certain spatial resolution to make changes visible and evident.

In Austria, continuous online UV monitoring started in 1998 on behalf of the Austrian Ministry of Environment by establishing the Austrian UV index network (45). So-called biometers have been utilized, which are broadband radiometers with erythema-like spectral sensitivity (Model 501, Solar Light Inc., USA; (46)). Locations of stations were selected by an objective method (47) in order to cover the whole country under special consideration of its geographical features, like the Alps. Today, the network consists of 13 stations and another 6 stations from neighboring countries participate in the online monitoring. These biometers mainly give information about the UVB range, due to their spectral response. So in a next step, the network was expanded by UVA broadband radiometers, which were placed aside the biometers at three stations. Today, at each of these stations, a UVA broadband radiometer measures global irradiance (sum of direct and diffuse radiation), while a second one is equipped with a shadow ring and only measures diffuse irradiance in parallel.

An important topic in monitoring is the quality of data and comparability. In this paper, we will introduce the applied methods for quality assurance and control including characteristics of instruments and calibration. Measurements and an analysis of global and diffuse UVA irradiance and daily radiant exposure (daily sums) will be presented for a period of up to 5 years, in order to indicate differences caused by location and local meteorology.

MATERIALS AND METHODS

Measuring sites. Three out of 13 stations of the Austrian UV network were equipped with UVA broadband radiometers (see Fig. 1), starting in 2013. The stations are located in Vienna (16.4°E, 48.3°N, 153 m a.s.l.), at the Kanzelhöhe Observatory (13.9°E, 46.7°N, 1540 m a.s.l.), which is located below the top of Mount Gerlitzen (1909 m a.s.l.), and in Kirchbichl (12.1°E, 47.5°N, 526 m a.s.l.). The latter is the substitute for the station in Innsbruck (11.4°E, 47.3°N, 577 m a.s.l.), which had to be moved because of technical reasons. The distance between Vienna and Mt. Gerlitzen, Vienna and Kirchbichl and Kirchbichl and Mt. Gerlitzen is 257, 333 and 167 km. Measurements started in May 2013 in Vienna (located in the flat planes in the East of the country), followed in July 2013 by Mt. Gerlitzen (located in the alpine South part), and by Innsbruck (July 2015), respectively, by the close-by Kirchbichl (June 2016, located in the West part, in an inner alpine valley of the river Inn). At each station, one instrument measures global irradiance and another one measures diffuse irradiance. In the last couple of months, two stations from Italy and two from Switzerland have also been delivering UVA measurements to the Austrian Network (see Fig. 1).

Instruments, properties and calibration. Three of the broadband radiometers (two located in Vienna and one in Kirchbichl) are of type J033 (CMS-Schreder, Austria). At Kirchbichl, the second broadband radiometer is of type WPD-UVA-03 (Gigahertz-Optik, Türkenfeld, Germany). At the Kanzelhöhe Observatory, two broadband radiometers of type UVS-AB-T (Kipp&Zonen, Delft, the Netherlands) are mounted.

As for any other broadband radiometer, special attention has to be paid to the raw measurements (e.g. 48), which are influenced by the properties of the instruments, such as spectral response or angular response.

The spectral response of these radiometers is shown in Fig. 2, together with the ideal UVA response. It can be seen that none of the instruments match the ideal UVA response perfectly and that there are obvious differences in the spectral response between the different types. Due to the usage of filters, slight differences in the spectral response occur within instruments of the same type. This is shown exemplarily for the UV-AB-T devices (dash-dot-dash line and the dash-dot-dot line).

As another example, the angular response of the broadband radiometers is not perfectly cosine-like and differs as well between the different types and between the instruments of the same type. Therefore, each instrument had to be characterized in the laboratory.

The formula below describes how the most critical properties of the device can be taken into account to gain a cosine responding UVA irradiance value from the output signal of the radiometer:

$$E\ [\mathrm{W\ m^{-2}}] = (\mathrm{S} - \mathrm{S0}) * \mathrm{c0} * \mathrm{c1}(\mathrm{O3}, \mathrm{se}) * \mathrm{c2}(\mathrm{se}, \mathrm{cl}) * \mathrm{c3}(T) * \mathrm{c4}(\mathrm{rH}) * \mathrm{c5}(\mathrm{S}) \quad (1)$$

S is the output signal and S0 is the dark signal. For all our radiometers, the signal is voltage. The dark signal is determined during night hours and assumed to be constant during the day. c0 is the conversion factor of the electrical signal under defined conditions (O3, sh, T, rH, S) in order to gain irradiance in W m^{-2}. c1 corrects for spectral changes of the solar spectrum, which result from solar elevation (se) and possibly from O_3 when the device is sensitive at shorter wavelengths. c2 corrects for deviations of the angular response from the ideal cosine response and from cloudiness (cl).

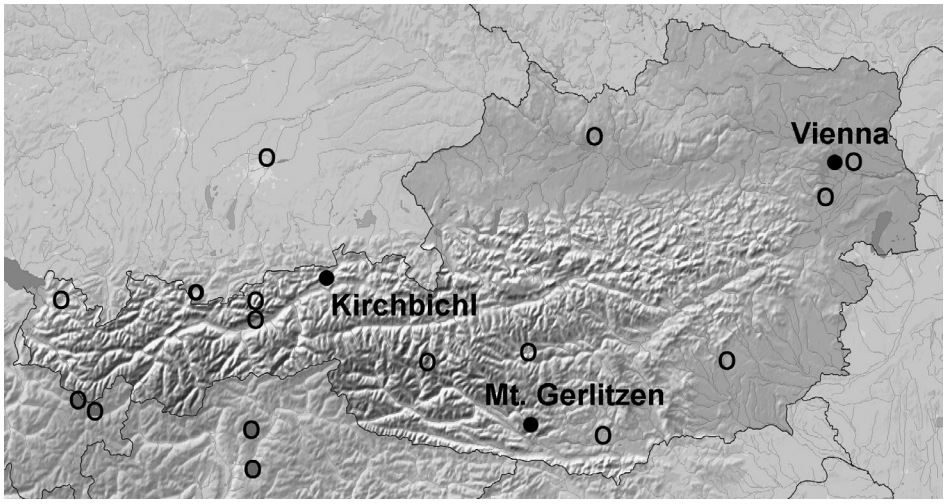

Figure 1. Stations of the Austrian UV network and participating stations from Germany, Italy and Switzerland. Black-filled circles indicate those stations in Austria where UVA and the UV index are measured and gray-filled circles those in Italy and Switzerland. Empty circles indicate stations where only the UV index is measured.

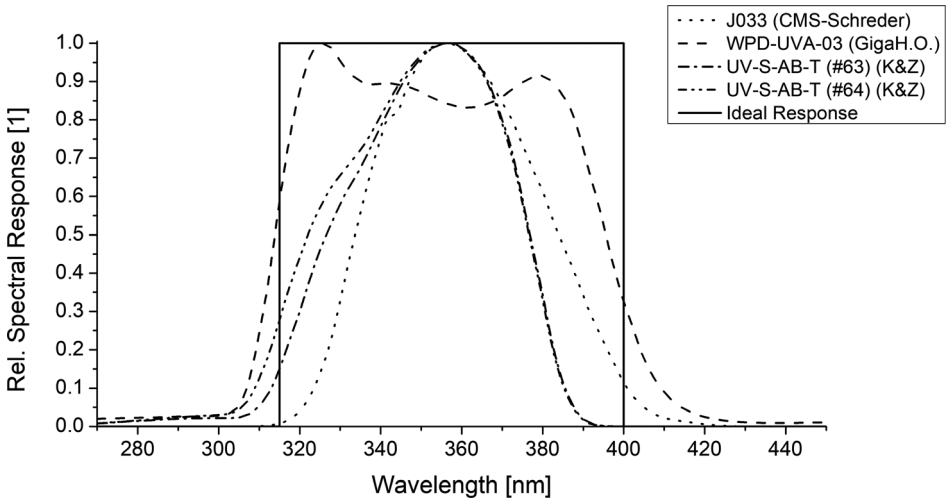

Figure 2. Spectral response of the broadband radiometers type J033 (CMS-Schreder), WPD-UVA-03 (Gigahertz-Optik) and UVS-AB-T (Kipp&Zonen) together with the ideal UVA response.

The influence of cloudiness on the cosine-correction c2 is considered by the method of calibration in front of the sun, where over several days with varying cloudiness, an average relation between the reference spectroradiometer and the broadband detector is derived (48). Therefore, in the application of Eq. (1), there remains only c2 (se).

c3 takes changes of sensitivity due to temperature (T) into account. c4 corrects for changes of sensitivity due to humidity (rH) and c5 corrects the deviation from linearity.

For the all three types of instruments, the factors c3, c4 and c5 can be assumed to be 1.0.

T (c3) and rH (c4) are kept constant, but not monitored. The frequency of replacement of the desiccant is based on long-term experience with broadband detectors. Linearity (c5) is not separately proofed, but during the comparisons with the reference spectroradiometer, no indication of nonlinearity was found.

Figure 3 exemplarily visualizes the calibration matrix for a radiometer of type J033, operating in Vienna. It takes into account the spectral c1 (O_3, se) and angular c2(se) response of the J033 which results in a dependence of solar elevation (spectral and angular response) and total ozone (spectral response). The resulting correction factor lies within 0.986 (500 DU, 50°) and 1.236 (200 DU, 0°). The correction factor references to 300 DU at solar elevation of 50° (c1(300DU, 50°) * c2 (50°) = 1).

Calibration of the instruments is carried out in front of the sun, whereas solar spectral irradiance is measured by the spectroradiometer in parallel. The calibrations in front of the sun are carried out for about 1 week with varying conditions of cloudiness in the time between May and August. There is no effect of the season, only the higher solar elevation in summer is desirable to cover the whole range of conditions during the year.

The expanded uncertainty of the derived UVA irradiance is estimated to be 6%, based on the uncertainty of the reference spectroradiometer and on the uncertainty of the characterization in the laboratory.

The devices are recalibrated every second year. The frequency of recalibration is based on long-term experience with broadband detectors. The calibration factors of some detectors are found to be stable over years, whereas for others, variations of 10% were observed from one calibration to the next. In summary, the recalibrations every 2 years show differences in the order of 5–10%. A linear drift of the calibration factor is assumed for the time between the calibrations, and the respective correction is applied to the measured data of this period.

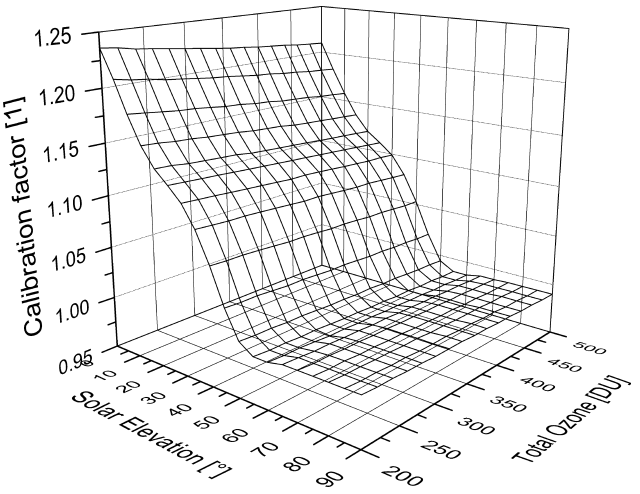

Figure 3. Calibration matrix c1(O_3, se) * c2 (se) according to Eq. (1) as a function of total ozone and solar elevation exemplarily for type J033 (#9822) operating in Vienna.

Diffuse radiation. At Mt. Gerlitzen, the UVA broadband radiometer for measuring diffuse irradiance is mounted on a sun tracker of type SOLYS2 (Kipp&Zonen, Delft, the Netherlands) together with a shadow ball to obstruct the solar disk.

At the two other sites, shadow-rings are utilized to block the direct solar radiation. In this case, no sun tracking device is needed, but the shadow-ring shields not only the solar disk but also a small part of the sky.

With that, the measurements E_{meas} are—by a certain percentage—too low and have to be corrected in order to receive the diffuse irradiance E_{diff}:

$$E_{diff} = E_{meas} * (1 + C_{SB}) \quad (2)$$

The amount of shielded irradiance—and with that correction factor C_{SB}—is the percentage of the upper hemisphere which is geometrically shadowed by the shadow-ring. Therefore, it depends on the radius and the width of the band, as well as the position of the sun (declination). For a shadow-ring with 7.5 cm width and a radius of 32 cm mounted at the station in Vienna, the C_{SB} values range from 2.7% (winter solstice) to 15.2% (summer solstice).

Measurements, availability, quality assurance and control. Measurements are carried out continuously—partly with a temporal resolution of 30 s—and mean values are stored every 1, 10 and 30 min. In this paper, we present the 30-min mean values.

The devices are checked by operators two to three times a week, whereas especially, the quartz domes of the devices are checked for dirt and dust, and the shadow-ring is adjusted. Moreover, three times a year all detectors are checked for humidity and the desiccant is renewed which assures that the broadband radiometers are dry during routine operation.

Approximately every 10 min, the measurements are transmitted to the Division of Biomedical Physics of the Medical University Innsbruck, where data are processed automatically in near real time. The calibration

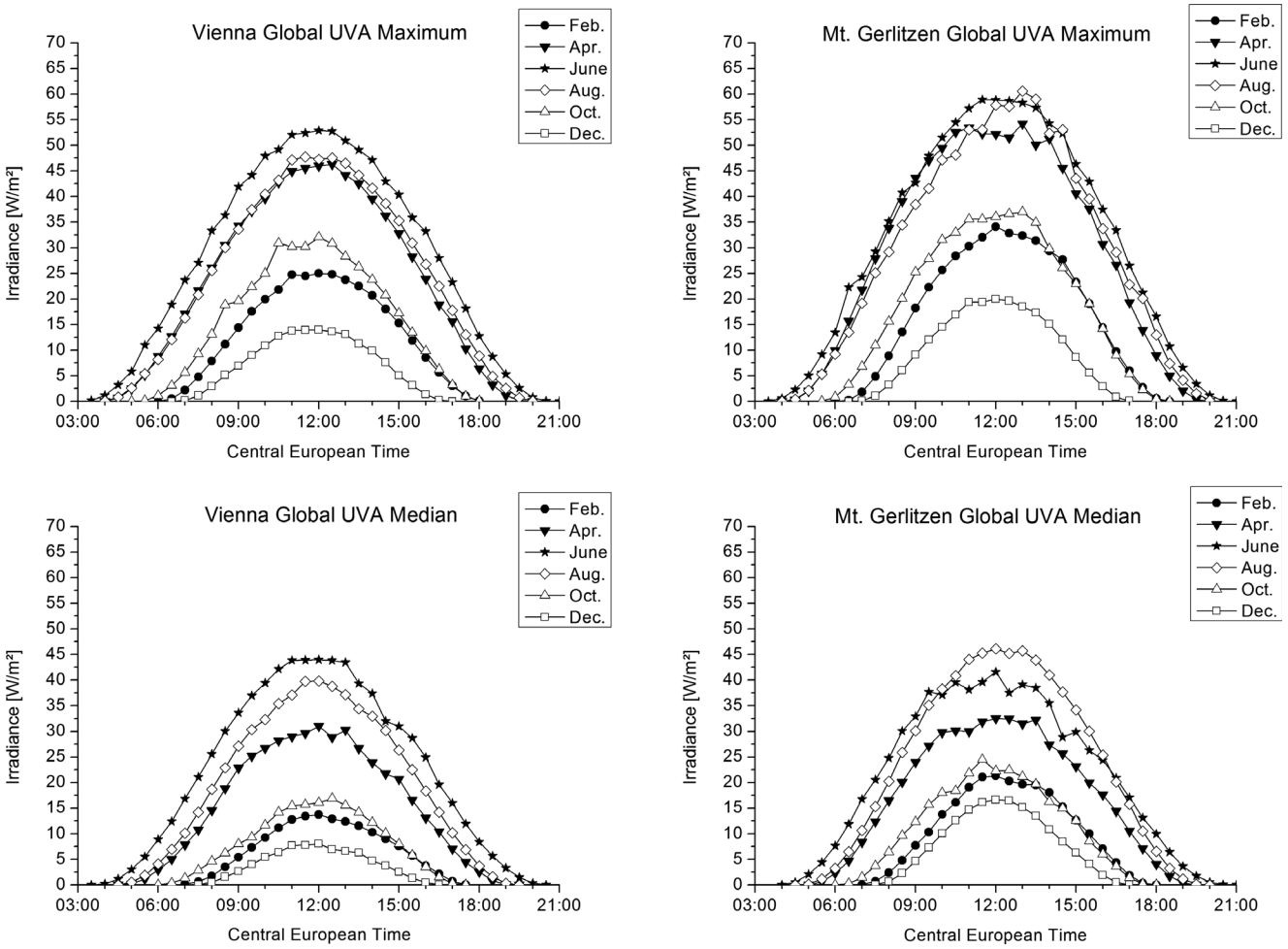

Figure 4. Maximum (upper panels) and median (lower panels) time courses of total UVA irradiance for every second month of the year at Vienna (left panels) and at Mt. Gerlitzen (right panels).

matrix is applied to the raw data, and the absolute values are then checked by comparison to clear sky model calculations. These are obtained by clear sky radiative transfer model UVSpec (49,50). As input for the model calculations (besides solar elevation, station altitude and climatological aerosol optical depth), the total ozone column is taken from the prediction of the NOAA Global Forecast System (GFS) and albedo is estimated from snow height information. By comparing the global UVA measurements to model calculations, outliers of over 20% above the modeled values are detected and eliminated (to compensate for the uncertainty in the model due to estimated input parameters). For diffuse UVA radiation, the global UVA measurements function as an upper boundary, again with a 20% tolerance.

Approximately 2 days after measurement, the analysis is repeated to take into account measured ozone values from OMI (NASA) instead of the forecast from NOAA. This procedure is the same for the UVA detectors and the erythemal detectors of the Austrian UV monitoring network. The correction following the publications of ozone measurements is relevant mainly for the erythemal detectors, whereas the UVA detector calibration is almost insensitive to small variations of the ozone content.

Once a new calibration is available, the whole data set starting from last year's calibration is reevaluated to consider the changes of the broadband radiometers during the 24 months that have been recovered.

Measurements are available online (www.uv-index.at), and they are updated every 10 min. Beside the recent value, the daily progress is visualized on the website. Additionally, the measurements of the previous day, the previous week as well as those of the last month and the last year are shown. A graph depicts the monthly maximum and the monthly mean values since measurements have started.

RESULTS

Daily course of global and diffuse UVA irradiance

Global UVA irradiance. Figure 4 provides the daily courses of maximum (upper panels) and median (lower panels) global UVA irradiance (as mean over 30 min) for every second month of the year at Vienna (left panels) and Mt. Gerlitzen (right panels), calculated from all available data.

The daily course of monthly maximum irradiance in Vienna (Fig. 4, upper left panel) shows similar values for May, June and July, but for August, values are noticeably lower. The highest values are on the order of 53 W m^{-2}. The lowest noon values occur in December ($\leq$14 W m^{-2}). The monthly medians (lower left panel) are highest in June and July, and they are up to 44 W m^{-2}. This denotes that the median values reach 83% of the maximum values in summer. In November, December and January, the median irradiance is lowest, staying below 8 W m^{-2}. With that, the median takes around 55% of the maximum value. This percentage is lower than that for summer, indicating more cloudy days in December compared to June or July.

At the alpine station Mt. Gerlitzen, the daily course of monthly maximum irradiance (Fig. 4, upper right panel) is highest in May, June, July and August, with values up to around 60 W m^{-2}. Maximum irradiance stays lowest in December ($\leq$20 W m^{-2}). Median values (lower right panel) are highest in July and August and may reach 45 W m^{-2}, which makes up 75% of the maximum. Lowest medians are found in November, December and January, reaching 17 W m^{-2}. With that, the winter median represents 83% of the winter maximum.

This indicates a clear difference between the alpine location Mt. Gerlitzen (1540 m a.s.l.) and Vienna (153 m a.s.l.), which is located in the plains (horizontal distance = 257 km). In Vienna, the summer is characterized by little cloud coverage, while high amounts of clouds are typical for winter. At Mt. Gerlitzen, the median is closer to the maximum during winter which denotes low cloudiness. Contrary to that, in summer, the ratio between median and maximum is lower, denoting a more frequent attenuation by clouds.

At Mt. Gerlitzen, the irradiance for cloudless sky (60 W m^{-2}) is approximately 12% higher than in Vienna (53 W m^{-2}). In respect to the difference of approximately 1390 m in altitude, this indicates an increase of UVA irradiance by 8–9% per 1000 m.

The data series for Kirchbichl (526 m asl), located in an inner alpine valley, is noticeably shorter than those from Vienna and Mt. Gerlitzen, so that the daily courses (especially the median) are not as smooth and expressive (and they are therefore not depicted). The highest values in June may reach 57 W m^{-2}, while in December, values are below 16 W m^{-2}. The median is highest in May and June, with values up to 50 W m^{-2} and lowest in December by staying below 13 W m^{-2}. The median in summer is 85% of the maximum, and in winter, it is 72%. With that, cloudiness in summer is similar to that in Vienna (83%) and in between the values of Mt. Gerlitzen (83%) and Vienna (55%) during winter.

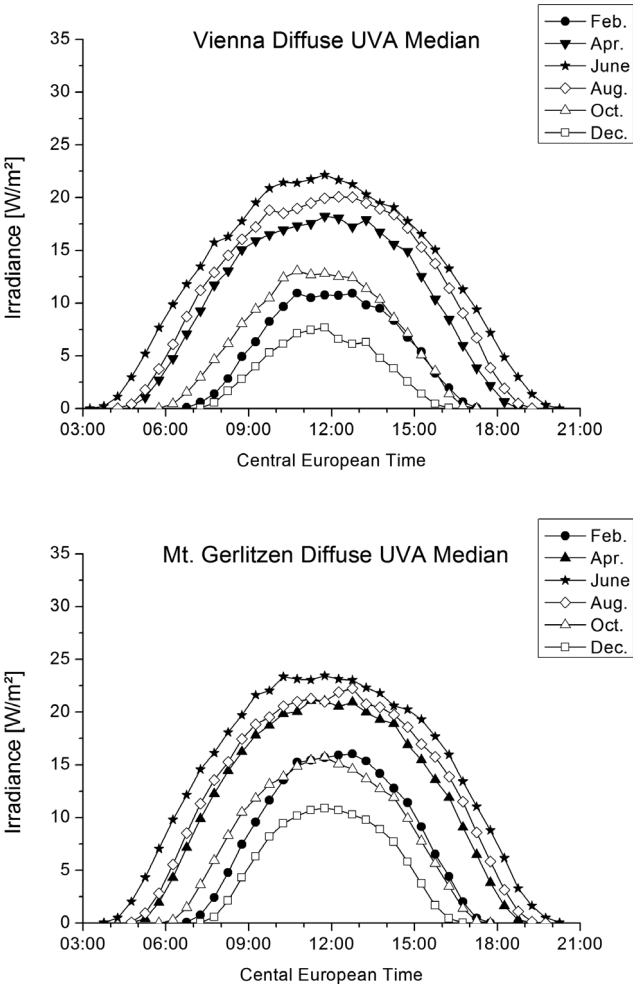

Figure 5. Daily courses of median diffuse UVA irradiance for every second month of the year at Vienna (upper panel) and Mt. Gerlitzen (lower panel).

Diffuse UVA irradiance. In Vienna, the median of diffuse irradiance (Fig. 5, upper panel) reaches 22 W m^{-2} at noon in the summer (May, June and July). In winter (December and January), it may reach 8 W m^{-2} and with that 35% of the summer median. Compared to the summer median of global irradiance (44 W m^{-2}), the diffuse median is 50%. In winter, the median of global and diffuse irradiance is almost the same (90%). This is another indicator for high cloudiness during winter.

At Mt. Gerlitzen, the summer median (Fig. 5, lower panel) of diffuse irradiance reaches 24 W m^{-2} (May, June and July) and stays below 11 W m^{-2} in December. With that, the winter median is 45% of that in summer. The comparison of the summer medians of diffuse and global UVA irradiance delivers a percentage of 53% for diffuse and a percentage of 65% when comparing the winter medians. This indicates noticeably less cloudy days in winter, compared to Vienna.

The daily courses (Figs. 4 and 5) visualize not only the change of irradiance throughout the year but also the changing length of the day. At the winter solstice, the sun is above the horizon for 8 h, and at the summer solstice, it is above the horizon for 16 h.

Ratio of global and diffuse irradiance. Under clear sky, the ratio between global and diffuse irradiance depends on a first order on solar elevation, respectively, the path length through the atmosphere. Figure 6 depicts the ratios during cloud-free days (selected by observers) at the observatory in Vienna (upper panel) and at the Kanzelhöhe observatory at Mt. Gerlitzen (lower panel). Both panels show the course during a day close to the summer solstice. The ratio decreases from 1 at sun rise to a value of around 0.4 at solar noon, where solar elevation is 65.0°, and increases back to 1 at sunset.

Under all sky conditions, cloud cover is the dominating factor for this ratio. Figure 7 visualizes the mean ratio for January (upper panel) and June (lower panel) at Vienna and Mt. Gerlitzen during the day. It can be seen that in January, the mean ratio in Vienna undergoes only a slight change: from around 1 at sunrise down to 0.90 at noon and back to 1 at dawn. At Mt. Gerlitzen, the ratio becomes lower at noon, decreasing to 0.73. In June, one can observe more pronounced courses compared to January, because clouds are less frequent. In Vienna, the mean ratio goes down to 0.54 while at Mt. Gerlitzen, it remains 10% higher

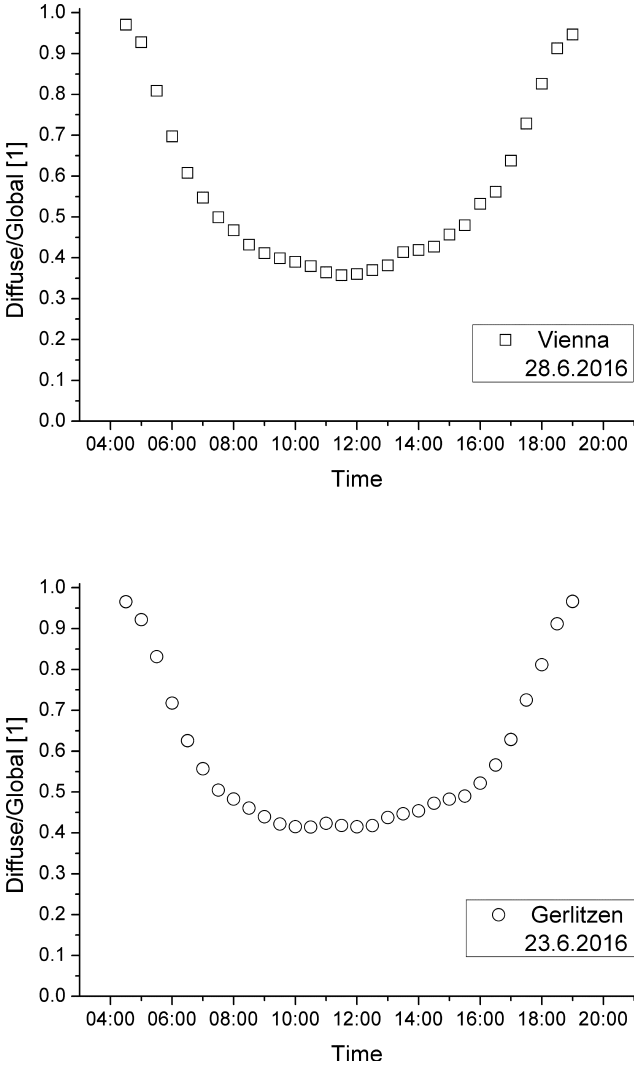

Figure 6. Ratio between diffuse and global UVA irradiance on cloud-free days close to summer solstice (solar elevation ≤ 65°) in Vienna (upper panel) and Mt. Gerlitzen (lower panel).

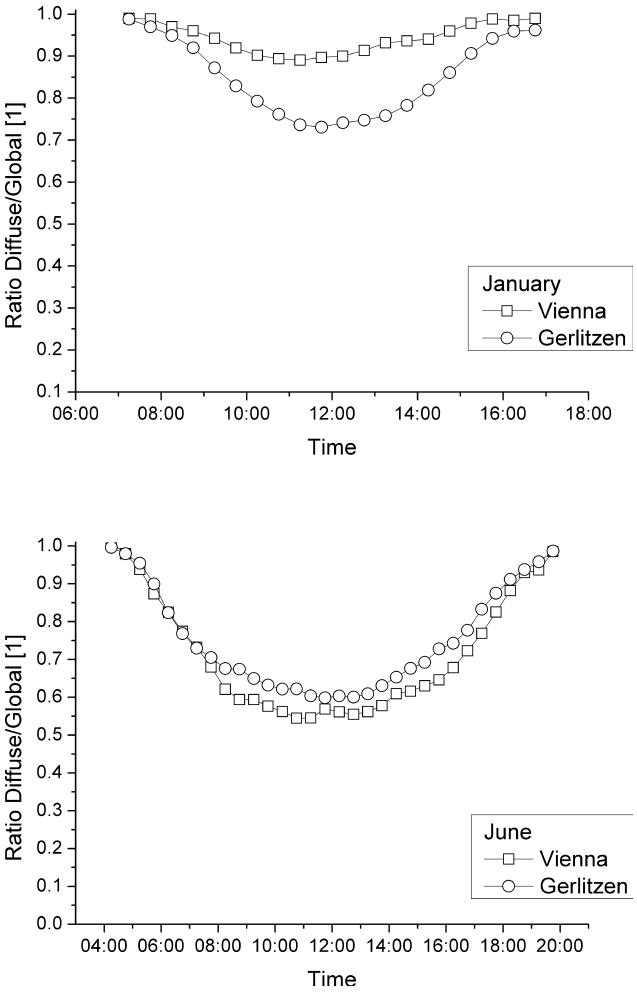

Figure 7. Time courses of the monthly mean ratio between diffuse and global UVA irradiance during the day at Vienna and Mt. Gerlitzen in January (upper panel) and June (lower panel).

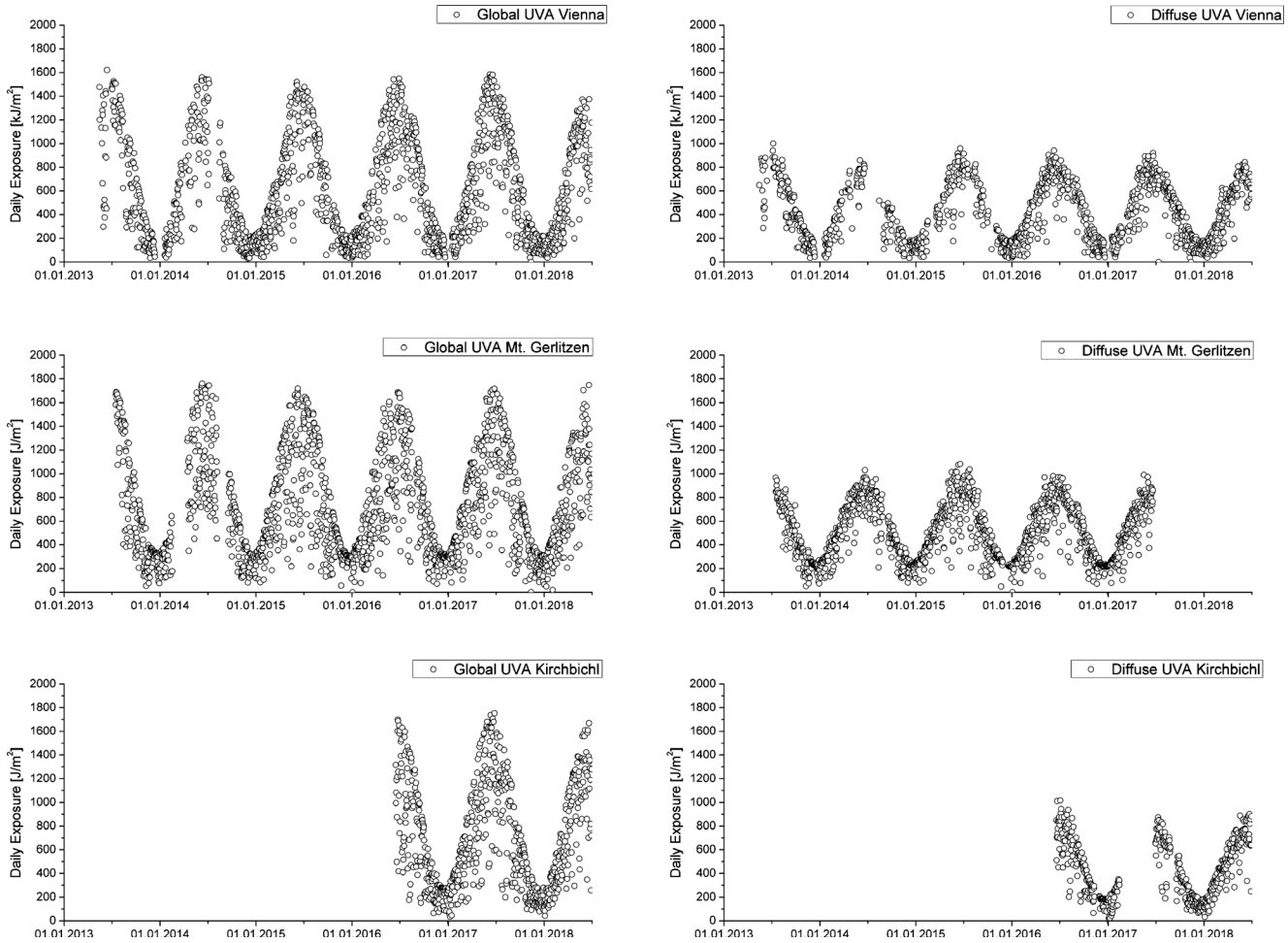

Figure 8. Daily global (left panels) and diffuse (right panels) UVA radiant exposure at Vienna (upper panels), Gerlitzen (middle) and Kirchbichl (lower panels).

(0.60). This denotes that there is less cloudiness in Vienna than that there is at Mt. Gerlitzen in June.

Daily UVA radiant exposure

Beside irradiance, the radiant exposure is an important photobiological factor. Figure 8 (upper left panel) depicts the global daily UVA radiant exposure (H_{GLO}) at Vienna over the whole period. A clear annual course can be recognized with lowest values between December and January and highest values in June. On a clear winter day, H_{GLO} may reach a value of 220 kJ m^{-2}, while in summer, H_{GLO} goes up to 1600 kJ m^{-2}, being seven times higher than in winter. The diffuse daily radiant exposure (H_{DIF}) (Fig. 8 upper right panel) mimics the course of H_{GLO}, but is noticeably lower in the summer. The annual course of radiant exposure is more pronounced than that of irradiance because in the summer, when irradiance is highest, the length of a day is up to twice as long as it is in winter, when irradiance is lowest. On a clear winter day (December to January), H_{DIF} may reach 190 kJ m^{-2}, which is just slightly below the global values. In summer, H_{DIF} may reach values around 900 kJ m^{-2}, which is around 56% of H_{GLO}.

The middle panels of Fig. 8 depict H_{GLO} and H_{DIF} at Mt. Gerlitzen over the whole period (the broadband radiometer for diffuse radiation failed in July 2017). At Mt. Gerlitzen, H_{GLO} in summer is 10% higher than in Vienna, reaching values of 1750 kJ m^{-2}. In December, the highest values go up to 320 kJ m^{-2}, representing one-fifth of the summer maximum. The lower panels of Fig. 8 show daily radiant exposure measurements for Kirchbichl.

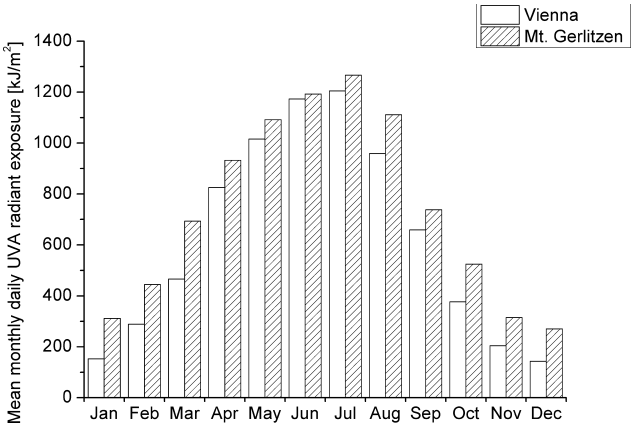

Figure 9. Monthly mean daily radiant exposure of global UVA radiation for Vienna and Mt. Gerlitzen.

Figure 9 depicts the monthly mean values of H_{GLO} at Vienna and Mt. Gerlitzen. Both distributions have an obvious skewness by peaking in July and lower values in the second half of the year compared to the first half of the year. This skewness results from the decrease in cloudiness in July compared to June that overwhelms the lower solar elevation and shorter length of the day. From September to November, more cloudiness reduces H_{GLO} compared to Spring. Comparing the values from Vienna and Mt. Gerlitzen, it can be seen that in June and July, the difference is only around 3%, although the altitude effect would cause 10–12%. In December and January, H_{GLO} at Vienna is just 50% of that measured at Mt. Gerlitzen. During winter, less cloudiness and the more frequent snow cover and corresponding enhanced albedo at Mt. Gerlitzen are responsible for this. Over the whole year, H_{GLO} is 17% lower at Vienna. This value deviates clear from that caused by the altitude effect.

DISCUSSION AND CONCLUSION

UVA cannot be reduced to the wavelength range between UVB and the visible spectral range. For several photobiological effects, it is the dominator either because of highest effectiveness of UVA radiation (e.g. pigmentation), or because of a higher irradiance in the UVA (e.g. like in the solar spectrum), which equalizes or overwhelms a higher effectiveness in the UVB (e.g. nonmelanoma skin cancer). Therefore, the UVA radiation has to be seen as an important measure that should be paid the same attention as UVB radiation or as global solar radiation.

Continuous monitoring of UVA radiation is carried out on a variety of locations around the world, but visibility for the scientific community and availability of recent data are rather restricted. The Austrian Federal Ministry for Sustainability and Tourism has attributed to these facts (importance and visibility) by ordering continuous high-quality measurements at three locations which have to be available online and free of charge.

In this paper, we have introduced the Austrian UVA network as well as with the applied procedures for calibration and quality assurance and control. Data from all stations indicate higher UVA radiant exposure in the first half of the year than in the second half because of a lower cloud amount in spring, compared to autumn. Further on, UVA radiant exposure shows seasonally alternating differences within relatively short distances caused by a change in altitude. In summer, decreased cloudiness in Vienna almost equalizes the altitude effect from 1400 m (to Mt. Gerlitzen). In winter, on the other hand, the UVA radiant exposure is almost twice as high at Mt. Gerlitzen as it is in Vienna. Responsible for this is a decrease in clouds and frequent snow coverage.

In comparison to the use of the more sophisticated spectroradiometers and spectrophotometers, using broadband radiometers for monitoring has several advantages (e.g. costs, less maintenance). However, broadband radiometers deliver integrated values over the whole wavelength range and differ in spectral sensitivity, and with that, the measurements of the same UVA source do. Therefore, special attention has to be put on calibration to gain irradiance values that are corrected for spectral and angular deviations from the ideal response. For broadband radiometers, which measure the UV index, standard calibration procedures (e.g. 51) are applied. However, there still seems to be a lack in application for UVA radiometers. We have randomly taken some examples from the literature to depict this problem: For a location at 31.9°N (54.4°E, 1230 m asl), a maximum daily radiant exposure up to 526 kJ m^{-2} in July was reported, respectively, up to 22 W m^{-2} at noon (52). Another study (30) at 31°N (35°E 300 m asl) states a mean value of 1460 kJ m^{-2} per day in June, respectively, 52 W m^{-2} on average at noon. A third study, which was carried out at a similar location (35.8°N, 33°E, 165 m asl), provides a mean daily radiant exposure of 820 kJ m^{-2} and 28 W m^{-2} at noon for July (31). With our calibration in respect to the angular response, spectral sensitivity and the changing solar spectrum, we gained maximum summer values on the order of 50–60 W m^{-2} at noon in Austria (46°N-48°N), respectively, daily integrals up to 1750 kJ m^{-2}.

The selected papers do not provide detailed information about calibration and certain doubt rises when comparing these values. Therefore, it is impossible to say whether differences between different locations are real or not. In these cases, inappropriate calibration leads to values that are simply not comparable and cannot be used for application. For example, solar UVA radiation is used in southern regions to disinfect drinking water (32) and UVA radiation measurements provide the necessary duration of irradiation to ensure disinfection. If calibration of instruments differs, the resulting duration of irradiation differs which may lead to a fail of disinfection.

RECOMMENDATION

For measurements of solar UVA radiation with broadband radiometers, we therefore strongly recommend the standard calibration as presented above (Chapter 2, Equation 1). This procedure is also obligatory for broadband radiometers measuring the UV index (3).

Acknowledgements—Installation and operation of the UV Monitoring network is funded by the Austrian Federal Ministry of Sustainability and Tourism.

REFERENCES

1. Gröbner, J. (2001) Characterisation of spectrophotometers used for spectral solar ultraviolet radiation measurements. *Radiat. Prot. Dosim.* **97**, 415–418.
2. WMO/GAW (2010) *Instruments to Measure Solar Ultraviolet Radiation Part 3: Multi-channel Filter Instruments*. GAW. Report no. 190, WMO/TD-No. 1537, WMO, Geneva, Switzerland.
3. Schmalwieser, A.W., J. Gröbner, M. Blumthaler, B. Klotz, H. De Backer, D. Bolsée, R. Werner, D. Tomsic, L. Metelka, P. Eriksen, N. Jepsen, M. Aun, A. Heikkilä, T. Duprat, H. Sandmann, T. Weiss, A. Bais, Z. Toth, A.M. Siani, L. Vaccaro, H. Diémoz, D. Grifoni, G. Zipoli, G. Lorenzetto, B.H. Petkov, A.G. di Sarra, F. Massen, C. Yousif, A.A. Aculinin, P. den Outer, T. Svendby, A. Dahlback, B. Johnsen, J. Biszczuk-Jakubowska, J. Krzyscin, D. Henriques, N. Chubarova, P. Kolarž, Z. Mijatovic, D. Groselj, A. Pribullova, J.R.M. Gonzales, J. Bilbao, J.M.V. Guerrero, A. Serrano, S. Andersson, L. Vuilleumier, A. Webb and J. O'Hagan (2017) UV Index monitoring in Europe. *Photochem. Photobiol. Sci.* **16**, 1349–1370.
4. Lubbock, Sir J. (1881) Observations on ants, bees, and wasps. VIII. Experiments with light of different wave-lengths. *J. Linn. Soc. Lond.* **15**, 362–387.
5. Lubbock, Sir J. (1882) On the sense of color among some of the lower animals. *J. Linn. Soc. Lond.* **16**, 121–127.
6. Schiemenz, F. (1924) Über den Farbensinn der Fische. *Z. Vergl. Physiol.* **1**, 175–220.

7. Wolff, H. (1925) Das Farbenunterscheidungsvermögen der Ellritze. *Z. Vergl. Physiol.* **3**, 279–329.
8. Goldsmith, T. H. (1981) Hummingbirds see near ultraviolet light. *Science* **207**, 786–788.
9. Arnold, K. and C. Neumeyer (1987) Wavelength discrimination in the turtle Pseudemys scripta elegans. *Vision. Res.* **27**, 1501–1511.
10. Jacobs, G. H., J. Neitz and J. F. Deegan (1991) Retinal receptors in rodents maximally sensitive to ultraviolet light. *Nature* **353**, 655–656.
11. Cronin, T. W. and M. J. Bok (2016) Photoreception and vision in the ultraviolet. *J. Exp. Biol.* **219**, 2790–2801.
12. Schmalwieser, A. W., S. Wallisch and B. Diffey (2012) A library of action spectra for erythema and pigmentation. *Photochem. Photobiol. Sci.* **11**, 251–268.
13. Brenner, M. and V. J. Hearing (2008) The protective role of melanin against UV damage in human skin. *Photochem. Photobiol.* **84**, 539–549.
14. Bissett, D. L., D. P. Hannon and T. W. Orr (1989) Wavelength dependence of histological, physical, and visible changes in chronically UV-irradiated hairless mouse skin. *Photochem. Photobiol.* **50**, 763–769.
15. Lavker, R. M., D. A. Veries, C. J. Irwin and K. H. Kaidbey (1995) Quantitative assessment of cumulative damage from repetitive exposures to suberythemogenic doses of UVA in human skin. *Photochem. Photobiol.* **62**, 348–352.
16. Lowe, N. J., D. P. Meyers, J. M. Wieder, D. Luftman, T. Borget, M. D. Lehman, A. W. Johnson and I. R. Scott (1995) Low doses of repetitive ultraviolet A induce morphological changes in human skin. *J. Invest. Dermatol.* **105**, 739–743.
17. McMillan, T. J., E. Leatherman, A. Ridley, J. Shorrocks, S. E. Tobi and J. R. Whiteside (2008) Cellular effects of long wavelength UV light (UVA) in mammalian cells. *J. Pharm. Pharmacol.* **60**, 969–976.
18. Sliney, D. H. (1995) UV radiation ocular exposure dosimetry. *J. Photochem. Photobiol., B* **31**, 69–77.
19. Roberts, J. E. (2011) Ultraviolet radiation as a risk factor for cataract and macular degeneration. *Eye Contact Lens.* **37**, 246–249.
20. Tuchinda, C., S. Srivannaboon and H. W. Lim (2006) Photoprotection by window glass, automobile glass, and sunglasses. *J. Am. Acad. Dermatol.* **54**, 845–854.
21. Kimlin, M. G. and A. V. Parisi (1999) Ultraviolet radiation penetrating vehicle glass: A field based comparative study. *Phys. Med. Biol.* **44**, 917–926.
22. Blumthaler, M., W. Ambach and R. Ellinger (1997) Increase of solar UV radiation with altitude. *Photochem. Photobiol. B* **39**, 130–134.
23. Löfgren, S. (2017) Solar ultraviolet radiation cataract. *Exp. Eye Res.* **156**, 112–116.
24. Grigalavicius, M., J. Moan, A. Dahlback and A. Juzeniene (2016) Daily, seasonal, and latitudinal variations in solar ultraviolet A and B radiation in relation to vitamin D production and risk for skin cancer. *Int. J. Dermatol.* **55**, e23–e28.
25. Hada, M., Y. Iida and Y. Takeuchi (2000) Action spectra of DNA photolyases for photorepair of cyclobutanepyrimidine dimers in sorghum and cucumber. *Plant Cell Physiol.* **41**, 644–648.
26. Sommer, R., M. Lhotsky, T. Haider and A. Cabaj (2000) UV inactivation, liquid-holding recovery, and photoreactivation of *Escherichia coli* O157 and other pathogenic *Escherichia coli* strains in water. *J. Food Prot.* **63**, 1015–1020.
27. Weihs, Ph., A.W. Schmalwieser and G. Schauberger (2012) UV effects on living organisms. In *Encyclopedia of Sustainability Science and Technology*, Vol. **16** (Edited by R. A. Meyers), pp. 11375–11427. Springer, New York, NY, USA.
28. Sagripanti, J. L. and C. D. Lytle (2007) Inactivation of influenza virus by solar radiation. *Photochem. Photobiol.* **83**, 1278–1282.
29. Moseley, H., M. Davison and R. M. MacKie (1983) Measurement of daylight UVA in Glasgow. *Phys. Med. Biol.* **28**, 589–597.
30. Kudish, A. I., V. Lyubansky, E. G. Evseev and A. Ianetz (2005) Statistical analysis and inter-comparison of the solar UVB, UVA and global radiation for Beer Sheva and Neve Zohar (Dead Sea), Israel. *Theor. Appl. Climatol.* **80**, 1–15.
31. Jacovides, C. P., F. S. Tymvios, D. N. Asimakopoulos, N. A. Kaltsounides, G. A. Theoharatos and M. Tsitouri (2009) Solar global UVB (280–315 nm) and UVA (315–380 nm) radiant fluxes and their relationships with broadband global radiant flux at an eastern Mediterranean site. *Agr. Forest Meteorol.* **149**, 1188–1200.
32. Sommer, B., A. Mariño, Y. Solarte, M. L. Salas, C. Dierolf, C. Valiente, D. Mora, R. Rechsteiner, P. Setter, W. Wirojanagud, H. Ajarmeh, A. Al-Hassan and M. Wegelin (1997) SODIS – An emerging water treatment process. *J. Wat. Supply Res. T.* **46**, 127–137.
33. Ubomba-Jaswa, E., C. Navntoft, M. I. Polo-López, P. Fernandez-Ibáñez and K. G. McGuigan (2009) Solar disinfection of drinking water (SODIS): An investigation of the effect of UV-A dose on inactivation efficiency. *Photochem. Photobiol. Sci.* **8**, 587–595.
34. Blumthaler, M., J. Gröbner, M. Huber and W. Ambach (1996) Measuring spectral and spatial variations of UVA and UVB sky radiance. *Geophys. Res. Letters* **23**, 547–550.
35. Blumthaler, M., W. Ambach and M. Salzgeber (1994) Effects of cloudiness on global and diffuse UV irradiance in a high-mountain area. *Theor. Appl. Clim.* **50**, 23–30.
36. Grant, R. H. and J. R. Slusser (2005) Estimation of ultraviolet-a irradiance from measurements of 368-nm spectral irradiance. *J. Atmos. Ocean Tech.* **22**, 1853–1863.
37. Sabburg, J., A. V. Parisi and J. Wong (2001) Effect of cloud on UVA and exposure to humans. *Photochem. Photobiol.* **74**, 412–416.
38. Chadyšiene, R. and A. Girgždys (2008) Ultraviolet radiation albedo of natural surfaces. *J. Environ. Eng. Landsc.* **16**, 83–88.
39. Bener, P. (1972) Final technical report No. DAJA 37-68-C-1017. Europ. Res. Office, U.S. Army, London, UK.
40. Reiter, R., K. Munzert and R. Sladkovic (1982) Results of 5-year concurrent recordings of global, diffuse and UV radiation at three levels (700, 1800 and 2999 m a.s.l.) in the Northern Alps. *Arch. Meteorol. Geophys. Biocl. B* **30**, 1–28.
41. Blumthaler, M., W. Ambach and W. Rehwald (1992) Solar UV-A and UV-B radiation fluxes at two Alpine stations at different altitudes. *Theor. Appl. Clim.* **46**, 39–44.
42. Piazena, H. (1996) The effect of altitude upon the solar UV-B and UV-A irradiance in the tropical Chilean Andes. *Sol. Energy* **57**, 133–140.
43. Simic, S., M. Fitzka, A. W. Schmalwieser, P. Weihs and J. Hadzimustafic (2011) Spectral dependency of UV radiation enhancements on clouds and surface albedo at Hoher Sonnblick. *Atmos. Res.* **101**, 869–878.
44. Williamson, C. E., R. G. Zepp, R. M. Lucas, S. Madronich, A. T. Austin, C. L. Ballaré, M. Norval, B. Sulzberger, A. F. Bais, R. L. McKenzie, S. A. Robinson, D.-P. Häder, N. D. Paul and J. F. Bornman (2014) Solar ultraviolet radiation in a changing climate. *Nat. Clim. Chang.* **4**, 434–441.
45. Blumthaler, M., B. Klotz, M. Schwarzmann and J. Schreder (2017) The Austrian UV monitoring network. *AIP Conf. Proc.* **1810**, 110001.
46. Berger, D. (1976) The sunburning ultraviolet meter: Design and performance. *Photochem. Photobiol.* **24**, 587–593.
47. Schmalwieser, A. W. and G. Schauberger (2001) A monitoring network for erythemally-effective solar ultraviolet radiation in Austria: Determination of the measuring sites and visualisation of the spatial distribution. *Theor. Appl. Climatol.* **69**, 221–229.
48. Blumthaler, M. (2004) Quality assurance and quality control methodologies within the Austrian UV monitoring network. *Rad. Prot. Dos.* **111**, 359–362.
49. Kylling, A., K. Stamnes and S.-C. Tsay (1995) A reliable and efficient two-stream algorithm for spherical radiative transfer: Documentation of accuracy in realistic layered media. *J. Atmos. Chem.* **21**, 115–150.
50. Mayer, B. and A. Kylling (2005) Technical note: The libRadtran software package for radiative transfer calculations – description and examples of use. *Atmos. Chem. Phys.* **5**, 1855–1877.
51. Webb, A., J. Gröbner and M. Blumthaler (2006) *A Practical Guide to Operating Broadband Instruments Measuring Erythemally Weighted Irradiance*. Office for Official Publications of the European Communities, Luxembourg.
52. Bouzarjomehri, F. and V. Tsapaki (2012) Measurement of solar ultraviolet radiation in Yazd, Iran. *Iran. J. Radiat. Res.* **10**, 187–191.